J Electr Eng Technol.2018; 13(2): 608-619
http://doi.org/10.5370/JEET.2018.13.2.608

ISSN(Print) 1975-0102
ISSN(Online) 2093-7423

Power Flow Algorithm for Weakly Meshed Distribution Network with Distributed Generation Based on Loop-analysis in Different Load Models

Hongsheng Su† and Zezhong Zhang*

Abstract – As distributed generation (DG) is connected to grid, there is new node-type occurring in distribution network. An efficient algorithm is proposed in this paper to calculate power flow for weakly meshed distribution network with DGs in different load models. The algorithm respectively establishes mathematical models focusing on the wind power, photovoltaic cell, fuel cell, and gas turbine, wherein the different DGs are respectively equivalent to PQ, PI, PQ (V) and PV node-type. When dealing with PV node, the algorithm adopts reactive power compensation device to correct power, and the reactive power allocation principle is proposed to determine reactive power initial value to improve convergence of the algorithm. In addition, when dealing with the weakly meshed network, the proposed algorithm, which builds path matrix based on loop-analysis and establishes incident matrix of node voltage and injection current, possesses good convergence and strong ability to process the loops. The simulation results in IEEE33 and PG&G69 node distribution networks show that with increase of the number of loops, the algorithm's iteration times will decrease, and its convergence performance is stronger. Clearly, it can be effectively used to solve the problem of power flow calculation for weakly meshed distribution network containing different DGs.

Keywords: Distributed Generation (DG), Load flow calculation, Weakly meshed distribution network, Loop-analysis

1. Introduction

In recent years, with the progress of electric power technology and the continued development of power industry, the distributed generation (DG) has been widely researched and applied. Different from the traditional power generation, DG can be dispersedly installed near the load, and also connected to distributed network, independently as in [1] and [2]. With aid of complementary and coordinated operation with DGs, electric power system can fully develop and utilize new energy resources to ensure the safety and reliability of the power-user. Hence, electric power experts believe that DG grid-connected can save investment, and reduce energy consumption, and also improve power supply reliability, such that it becomes the developmental direction of electric power industry in 21st century [3-6].

Power flow calculation of distribution networks is the basis of other advanced respects, such as reactive power optimization, network planning and reconfiguration, capacitor and DG placement, and etc [7-9]. There are differences between distribution network and transmission network in the aspect of structure, that is, high voltage transmission system generally adopts multiple loops structure, whereas distribution system uses the radiant or weakly meshed structure [10]. The normal operation of distribution network is in open loop way, and both sides of the contact switch are equivalent to the end of feeder. As outage of one side, the other side will transmit electric energy, inversely. Moreover, in the actual operation, load power will change with the change of voltage such that the distribution of power flow will be different along with various load models. If the load voltage caused by disturbance of DG can not be maintained in range of the permitted scope, the voltage of power system may be instable as in [11] and [12]. Therefore, it is important to research power flow calculation for weakly meshed network containing DGs and considering its load characteristics.

Several investigations have been conducted on power flow calculation of distribution networks with DGs. In [13], a distributed slack bus model is presented applying the concept of generator domains for DGs in unbalanced power flow. Considering the existence of weak circuit loops, some algorithms to calculate the power flow of weakly meshed distribution networks have already been reported in [14-16], wherein some advanced technologies have already been adopted, for instance, fuzzy technology [14], object-oriented technology [15]. Zbus method and forward/backward sweep method are combined to calculate power flow for weakly meshed distribution network in

† Corresponding Author: School of Automation and Electrical Engineering, Lanzhou Jiaotong University, China; Rail Transit Electrical Automation Engineering Laboratory of Gansu Province, Lanzhou Jiaotong University, China. (suhs@mail.lzjtu.cn)
* School of Automation and Electrical Engineering, Lanzhou Jiaotong University, China. (980222656@qq.com)
Received: May 1, 2017; Accepted: November 13, 2017

[16], where the network is divided into radiant structure and annular one, wherein radiant structure uses forward/ backward sweep method, whereas annular structure uses Zbus method to deal with power flow calculation for weakly meshed distribution network. But the algorithm does not consider the situation of DG grid-connected. Considering the existence of PV-type DGs, the traditional power flow algorithms are improved to calculate the power flow of distribution networks with multiple DGs [17-20]. However, those methods can not calculate the power flow of distribution networks with weak circuit loops. In [21], an algorithm is presented for the calculation power flow which uses the sensitivity compensation method to compensate the voltage deviation through PV nodes. In [22], the back/forward sweep algorithm is adopted to perform power flow calculation for distributed network with DGs. With the introduction of virtual node insulating from PV node, the algorithm takes advantage of the sensitivity impedance matrix to process virtual nodes to make the voltage amplitude and injection active power of virtual node consistent with that of PV node, but they can not reflect the capacities of DGs and load, which generates some influences on distribution networks losses in different levels of DG penetration. In actual cases, the load power is closely related to the voltage. The constant power load model can not accurately reflect the distribution of power flow.

To aim at the deficiencies that traditional power flow algorithms can not solve power flow calculation for distribution networks containing DGs, based on the static load characteristics, this paper proposes an efficient power flow calculation for weakly meshed distribution network with different types of DGs. The algorithm respectively establishes mathematical models focused on the wind power, photovoltaic cell, fuel cell, and gas turbine. When dealing with PV node, it adopts reactive power compensation device to correct power, and the reactive power allocation theory to determine reactive initial values. In addition, when dealing with the weakly meshed network, the proposed algorithm, which builds path matrix based on loop-analysis, and establishes incident matrix of node voltage and injection current, has good convergence and strong ability to process the loops. The simulation results in IEEE33 and PG&G69 node distribution networks show that the proposed algorithm is effective and feasible.

2. Distributed Network Model Containing DG

Power flow calculation is a significant project to evaluate its operating performance after DG is grid-connected. In general, distributed grids contain two-type node, that is, power supply node and load node. The former can be seen as balance node, and the latter as PQ node. Since the location of the DG is typically near the load center, here we assume that the DG is installed on the load node as shown in Fig. 1.

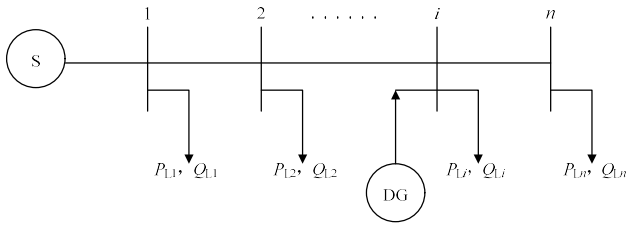

Fig. 1. Single radiant circuit with a DG

From Fig. 1, there is a DG installed in its *i*th load-node of the line with active power being P_{Li} and reactive power being Q_{Li}, where P_{DGi} and Q_{DGi} for DG. For the bus *i* of the *i*th node, the active power flow can be divided as three-kind condition: as $P_{DGi} > P_{Li}$, the node injects the power into the grid and is seen as power supply node; as $P_{DGi} < P_{Li}$, the node absorbs the power from the system, and is seen as load node; if $P_{DGi} = P_{Li}$, and the node may be seen as balanced node. Clearly, in the former two cases, there are power flowing between the grid and load node, and for the last case, this is not exists. Moreover, we also note that there will generate diverse influence on the gird as the DG is located at diverse sites, say, the line loss will reduce and the voltage can increase as the DG is installed at end node, and conversely, if the DG is located at substation node, the capacity of the substation will be expanded whereas the line load capacity does not obtain ascension. Clearly, the site and size of the DG access will have large influence on the system.

According to [23], usually, the following several issues worthy to note when the DGs are accessed to distributed networks.

1) When the capacity of the DG access system is less than or equal to the one of the total load in distributed system, the DG will reduce the loss of the distribution network.
2) When the capacity of the DG access system is less than or equal to the one of the total access load in distributed system, but there is one or several DGs capacity is greater than the load of the access node, and then the DG still possesses the effect to reduce network loss.
3) There is the capacity of one or more DGs larger than the load of the access node, but if the total capacity of all the access DGs is more than the whole system load, and less than twice the total load, under this kind of situation, the DG can reduce the loss of system like 2). However, if the total capacity of all DGs in the system is greater than twice the total load of the whole system, then DG not only fails to reduce the network loss, but also increases the loss of the system.

3. Power Flow Calculation Model of DG

Generally, traditional distribution network includes balance node and PQ nodes, wherein bus-bar of substation export is regarded as balance node or power source node,

and the other nodes including load node and intermediate node are regarded as PQ nodes. With DG grid-connected, the system will appear new node type [24].

3.1 Wind power generation

Wind generators usually include asynchronous generator and synchronous generator, wherein the asynchronous ones have been widely used, and are equivalent to PQ(V) nodes. When processing the PQ(V) node, the active power is regarded as constant [11]. The function between voltage and reactive power can be described by

$$Q_{DG} = -\frac{U^2}{X_P} + \frac{-U^2 + \sqrt{\mathrm{U}^4 - 4\mathrm{P}_{DG}^2\mathrm{X}^2}}{2\mathrm{X}} \tag{1}$$

where X_{P} expresses sum of stator leakage resistance and rotor leakage resistance, and X is the excitation reactance, and P_{DG} and U are respectively the active power output of DG and the voltage of the machine.

The synchronous generator is equivalent to PQ node, known as "negative load," and described by

$$\begin{cases} P_L = -P_{DG} \\ Q_L = -Q_{DG} \end{cases} \tag{2}$$

3.2 Fuel cell

Fuel cell is a kind of device with high conversion efficiency and small pollution to the environment that makes chemical energy stored in fuel and oxidant transformed into electrical energy. In power flow calculation, fuel cell can be equivalent to PV node [25]. If the reactive power is out-of--limit, it will be converted as PQ node to process.

3.3 Photovoltaic cell

Equivalent Circuit of photovoltaic cell is shown in Fig. 2.

When accessed to the load, the relationship among load current I and I_{PH}, I_D, I_{SH} can be expressed by

$$\mathrm{I} = \mathrm{I}_{\mathrm{PH}} - \mathrm{I}_{\mathrm{D}} - \mathrm{I}_{\mathrm{SH}} \tag{3}$$

The relationship between load voltage V and diode voltage V_{D} can be expressed by

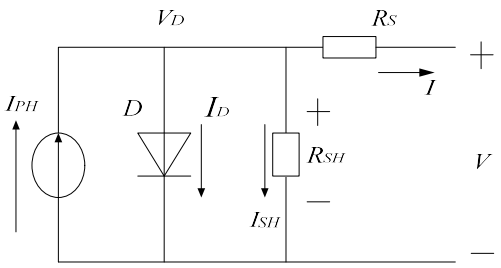

Fig. 2. Equivalent circuit of photovoltaic cell

$$\mathrm{V} = \mathrm{V}_{\mathrm{D}} - \mathrm{R}_{\mathrm{S}} \times \mathrm{I} \tag{4}$$

Photovoltaic cell can be controlled by inverter for reactive power compensation. When the inverter is the current source inverter, the active power output of photovoltaic cell and injection current are constant. To track the change of power system voltage by controlling the output current of inverter can achieve the goal of grid-connected operation [26]. Therefore, photovoltaic cell equals to PI node, and the function of reactive power can be established by

$$\mathrm{Q}_{DG} = \sqrt{|\mathrm{I}|^2 (\mathrm{e}^2 + \mathrm{f}^2) - \mathrm{P}_{DG}{}^2} \tag{5}$$

where I is the injection current of distribution network, e and f respectively is real part and imaginary part of DG voltage, P_{DG} is the active power output.

When the inverter is voltage controlled model, the photovoltaic cell is equivalent to PV node.

3.4 Micro gas turbine

Micro gas turbine is rotary heat engine with fuel and air as medium. In power flow calculation, it is equivalent to PV node [25]. If it is out-of-limit in the calculation, it will be converted as PQ node.

4. Static Load Characteristics Models

According to [27], the response of loads to voltage changes occurring over many minutes can affect voltage stability. Especially, for transient voltage stability, the dynamic characteristics of loads such as induction motors are critical. In some systems, there are enough control devices to keep loads constant, and the load characteristics are then unimportant until the controls reach limits. In large-scale simulation, constant power loads are usually represented on the high voltage side of bulk power delivery substations; the neglect of transformer and feeder impedances may compensate for the conservative constant power assumption, such that it is reasonable for approximate static analysis when a significant of the loads is motors. The alternative to constant power load models is representation of voltage sensitive loads plus regulators which restore load.

In [28], the voltage sensitivity for static models is in exponential form:

$$\begin{cases} \mathrm{P}_L = \mathrm{P}_0 \left(\dfrac{\mathrm{U}_\mathrm{i}}{\mathrm{U}_N} \right)^{\alpha} \\ \mathrm{Q}_L = \mathrm{Q}_0 (\dfrac{\mathrm{U}_\mathrm{i}}{\mathrm{U}_N})^{\beta} \end{cases} \tag{6}$$

where P_0 and Q_0 respectively represent active power

and reactive power under the rated voltage, and U_i is actual voltage, and U_N represents rated voltage, and α and β are respectively load characteristics coefficients of active power and reactive power, and $\alpha=\beta=0$, $\alpha=\beta=1$, $\alpha=\beta=2$ represent the constant power, constant current and constant impedance load model, respectively.

There static models may be valid for only a limited voltage range(say, ±10%). For large voltage deviations, the representation of loads by exponential models with exponential value less than 1.0 in dynamic simulation is inadequate, such as motors and lightings [27].

In (6), the α and β terms can be understand as thatα is the $\triangle P$ for a $\triangle U$ and β is the $\triangle Q$ for a $\triangle U$. we can show this using a two-term binomial expansion of Eq. (6) by

$$\begin{cases} \alpha = \dfrac{\Delta P}{\Delta U} \\ \beta = \dfrac{\Delta Q}{\Delta U} \end{cases} \quad \text{with } P_0 = U_N = 1 \text{ pu} \tag{7}$$

For the examples in this paper, since the capacity of access DGs is quite small compared with one of the loads of the whole distributed network, and only scattered in several nodes, the scope of the voltage deviations affected by it will not very large. Hence, it should be adequate to consider the static model.

5. PV-node Processing

5.1 Calculation of reactive power revised

Assuming that there are *n* PV-type DGs accessed to distributed network, and the injection current direction of DG is the positive direction, the function of node voltage increment matrix $\Delta \overline{\boldsymbol{U}}$ is then expressed by

$$\boldsymbol{Z}\,\Delta \overline{\boldsymbol{I}} = \Delta \overline{\boldsymbol{U}} \tag{8}$$

where $\Delta \overline{\boldsymbol{I}}$ is the node current increment matrix, and $\boldsymbol{Z}$ is node impedance matrix of DG. Node power increment is represented by

$$\Delta \overline{\boldsymbol{S}} = \boldsymbol{U}\,\Delta \overline{\boldsymbol{I}}^{*} \tag{9}$$

where $\Delta \overline{\boldsymbol{S}}$ is node power increment matrix, and $\boldsymbol{U}$ is node voltage matrix, and $\Delta \overline{\boldsymbol{I}}^{*}$ is conjugate matrix of $\Delta \overline{\boldsymbol{I}}$.

Under the normal operation of distribution network, the difference of voltage magnitude and phase angle is small, for ease of calculation, per unit of node voltage approximately equals to 1, Eq. (9) can be written as

$$\Delta \overline{\boldsymbol{S}}^{*} \approx \Delta \overline{\boldsymbol{I}} \tag{10}$$

Substituting (10) into (8), we obtain

$$\Delta \overline{\boldsymbol{U}} \approx \boldsymbol{Z}\,\Delta \overline{\boldsymbol{S}}^{*} \tag{11}$$

wherein $\Delta \overline{\boldsymbol{U}}$ mainly depends on the real part $\Delta \boldsymbol{U}$.

Let $\boldsymbol{Z} = \boldsymbol{R} + \boldsymbol{jX}$ and $\Delta \overline{\boldsymbol{S}}^{*} = \Delta \boldsymbol{P} - \boldsymbol{j}\Delta \boldsymbol{Q}$, and then substitute it into (11), so that the real part of Eq.(11) can be obtained by

$$\boldsymbol{R}\,\Delta \boldsymbol{P} + \boldsymbol{X}\,\Delta \boldsymbol{Q} = \Delta \boldsymbol{U} \tag{12}$$

Due to the constant active power of PV-type DG, namely $\Delta \boldsymbol{P}$ for 0, Eq. (12) can be simplified as

$$\boldsymbol{X}\,\Delta \boldsymbol{Q} = \Delta \boldsymbol{U} \tag{13}$$

where $\boldsymbol{X}$ is node reactance matrix.

Hence, the revised value of reactive power is

$$\Delta \boldsymbol{Q} = \boldsymbol{X}^{-1}\,\Delta \boldsymbol{U} \tag{14}$$

where $\boldsymbol{X}^{-1}$ is inverse matrix of $\boldsymbol{X}$.

Eq. (14) shows that the reactive power correction matrix $\Delta \boldsymbol{Q}$ of PV-type DG not only relate to inverse matrix of node impedance matrix and voltage deviation, but also relate to other nodes of system. Voltage deviation is gotten by the voltage difference of iteration before and after.

5.2 Derivation process of node reactance matrix

Assuming that $\boldsymbol{X}$ called node reactance matrix is a $n \times n$ -order square symmetric matrix. Its elements are made of node reactance value. The diagonal element is called self-reactance, and non-diagonal element is called mutual reactance [29]. There are two DGs respectively accessed in node 5 and 11 in Fig. 3. The calculating process of each element is shown by

$$\boldsymbol{X} = \begin{pmatrix} x_{11} & x_{12} \\ x_{21} & x_{22} \end{pmatrix} \tag{15}$$

$$\begin{cases} x_{11} = X_1 + X_2 + X_3 + X_5 \\ x_{22} = X_1 + X_2 + X_3 + X_6 + X_{11} \\ x_{12} = x_{21} = X_1 + X_2 + X_3 \end{cases} \tag{16}$$

where X_n represents for reactance value of node *n*, and x_{11}, x_{22} are self-reactance, and x_{12}, x_{21} are mutual reactance.

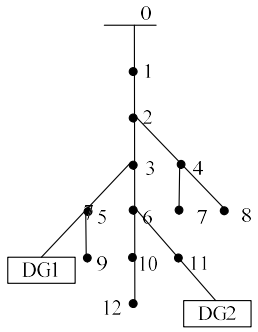

Fig. 3. Distribution power system with DGs

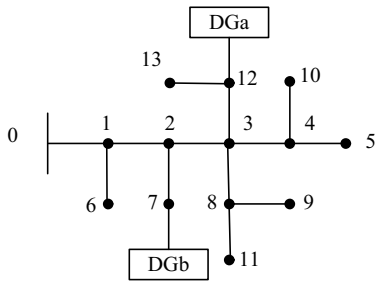

Fig. 4. Distribution power system

5.3 Calculation of initial value of reactive power

When solving the power flow calculation of PV-type node, reactive initial value of PV node should be set. Large deviation between the reactive initial value from the traditional method and the actual value leads to increasing iterations, so reactive power allocation theory [30] is considered to determine the reactive initial value, which clearly can improve the convergence of algorithm.

Reactive power of PV-type DG is provided by the reactive power compensation device, assuming that reactive power compensation device is infinity, reactive power value is obtained by node impedance matrix, and it is not only related to the position of DG, but also related to load size and location. Therefore, reactive initial value can be divided into two parts. Firstly, selecting the branch which has maximum reactive power value from power source node to DG, then, determining the first part which is half of the total reactive power of load from power source node to PV node, and the other part is sum of the reactive power from PV node to end node.

As shown in Fig. 4, PV-type DG a and b are respectively installed at node 12 and node 7, the reactive initial value of the two DGs are below.

$$Q_a = (Q_1 + Q_2 + Q_3)/2 + (Q_{12} + Q_{13}) \tag{17}$$

$$Q_b = (Q_1 + Q_2)/2 + Q_7 \tag{18}$$

where Q_a and Q_b are reactive initial values of the distributed generations, and Q_n is reactive power of the node n (n=1,2,…,13). In actual situation, the capacity of reactive power compensation device can not reach infinity, so if the initial value is greater than the maximum capacity of compensation device, reactive initial power value will be revised to the maximum capacity value of compensation device.

6. Power Flow Calculation of Weakly Meshed Distribution Network

6.1 Handling of weakly meshed network

Weakly meshed distribution network with the first node as the reference node has N nodes, b branches and m independent loops. The number of independent nodes and branches are n (n =N-1) and b (b =n +m). The basic loop - branch incident matrix describes the relationship between basic loops, tree branches, and link branches. $\boldsymbol{B}$ is a $m \times b$ - order loop-branch incident matrix. $\boldsymbol{T}$ is a $n \times b$ -order path-branch incident matrix [31].

From Kirchhoff's Current Law, we can obtain

$$\mathbf{B}^T\mathbf{I}_1 + \mathbf{T}^T\mathbf{I}_g = \mathbf{I}_b \tag{19}$$

where $\mathbf{I}_b$ is a $b \times 1$ -order branch current matrix, and $\mathbf{I}_g$ is a $n \times 1$ -order node injection current matrix, and $\mathbf{I}_1$ is a $m \times 1$ -order loop current matrix.

The branch and the loop are respectively used Ohm's Law and Kirchhoff's Voltage Law, then

$$\mathbf{U}_b = \mathbf{Z}_b\mathbf{I}_b \tag{20}$$

$$\mathbf{B}\mathbf{U}_b = \mathbf{0} \tag{21}$$

where $\mathbf{U}_b$ is a $b \times 1$ -order branch voltage matrix, $\mathbf{Z}_b$ is a $b \times b$ -order branch impedance diagonal matrix.

Based on corresponding tree branch and link branch, $\boldsymbol{T}$ and $\boldsymbol{B}$ can be described by

$$\mathbf{T} = \begin{bmatrix}\mathbf{T}_t & \mathbf{T}_1\end{bmatrix} = \begin{bmatrix}\mathbf{T}_t & \mathbf{0}\end{bmatrix} \tag{22}$$

$$\mathbf{B} = \begin{bmatrix}\mathbf{B}_t & \mathbf{B}_1\end{bmatrix} = \begin{bmatrix}\mathbf{B}_t & \mathbf{E}_m\end{bmatrix} \tag{23}$$

where T_1=0, since link branch does not belong to any path. The direction of loop is consistent with that of link branch, so $\mathbf{B}_1 = \mathbf{E}_m$ and $\mathbf{E}_m$ is a m×m-order identity matrix. Similarly, $\mathbf{I}_b$ can be decomposed into $\mathbf{I}_{bt}$ (n×1-order matrix) and $\mathbf{I}_{b1}$ ($m \times 1$ -order matrix) ($\mathbf{I}_{b1} = \mathbf{I}_1$), $\mathbf{U}_b$ can be decomposed into $\mathbf{U}_{bt}$ ($n \times 1$ -order matrix) and $\mathbf{U}_{b1}$ ($m \times 1$ - order matrix), $\mathbf{Z}_b$ can be decomposed into $\mathbf{Z}_{bt}$ ($n \times 1$ -order matrix) and $\mathbf{Z}_{b1}$ ($m \times 1$ -order matrix). In conclusion, Eq. (21) can be expanded by

$$\begin{aligned}\boldsymbol{B}\boldsymbol{U}_b &= \begin{bmatrix}\boldsymbol{B}_t & \boldsymbol{E}_m\end{bmatrix}\begin{bmatrix}\boldsymbol{U}_{bt} \\ \boldsymbol{U}_{b1}\end{bmatrix} = \begin{bmatrix}\boldsymbol{B}_t & \boldsymbol{E}_m\end{bmatrix}\begin{bmatrix}\boldsymbol{Z}_{bt} & \boldsymbol{0} \\ \boldsymbol{0} & \boldsymbol{Z}_{bt}\end{bmatrix}\begin{bmatrix}\boldsymbol{I}_{bt} \\ \boldsymbol{I}_{b1}\end{bmatrix} \\ &= \begin{bmatrix}\boldsymbol{B}_t & \boldsymbol{E}_m\end{bmatrix}\begin{bmatrix}\boldsymbol{Z}_{bt} & \boldsymbol{0} \\ \boldsymbol{0} & \boldsymbol{Z}_{b1}\end{bmatrix}\begin{bmatrix}\boldsymbol{T}_t^T & \boldsymbol{B}_t^T \\ \boldsymbol{0} & \end{bmatrix}\begin{bmatrix}\boldsymbol{I}_g \\ \boldsymbol{I}_1\end{bmatrix} = \boldsymbol{0}\end{aligned} \tag{24}$$

$$\begin{aligned}\boldsymbol{B}\boldsymbol{U}_b &= \boldsymbol{B}_t\boldsymbol{U}_{bt} + \boldsymbol{U}_{b1} = \boldsymbol{B}_t\boldsymbol{Z}_{bt}\boldsymbol{I}_{bt} + \boldsymbol{Z}_{bt}\boldsymbol{I}_{b1} \\ &= \boldsymbol{B}_t\boldsymbol{Z}_{bt}\boldsymbol{T}_t^T\boldsymbol{I}_g + (\boldsymbol{B}_t\boldsymbol{Z}_{bt}\boldsymbol{B}_t^T + \boldsymbol{Z}_{b1})\boldsymbol{I}_1 = \boldsymbol{0}\end{aligned} \tag{25}$$

$$\mathbf{I}_{bt} = \mathbf{T}_t^T\mathbf{I}_g + \mathbf{B}_t^T\mathbf{I}_1 = \mathbf{f}_1 + \mathbf{f}_2 \tag{26}$$

where $\mathbf{f}_1 = \mathbf{T}_t^T\mathbf{I}_g$, $\mathbf{f}_2 = \mathbf{B}_t^T\mathbf{I}_1$. From (25), we obtain

$$\mathbf{B}_t\mathbf{Z}_{bt}\mathbf{T}_t^T\mathbf{I}_g + (\mathbf{B}_t\mathbf{Z}_{bt}\mathbf{B}_t^T + \mathbf{Z}_{b1})\mathbf{I}_1 = \mathbf{0} \tag{27}$$

where $\mathbf{B}_t\mathbf{Z}_{bt}\mathbf{B}_t^T + \mathbf{Z}_{b1} = \mathbf{B}\mathbf{Z}_b\mathbf{B}^T = \mathbf{Z}_1$, and $\mathbf{Z}_1$ is the loop impedance matrix.

$$\boldsymbol{I}_1 = -\boldsymbol{Z}_1^{-1}\boldsymbol{B}_t\boldsymbol{Z}_{bt}\boldsymbol{T}_t^T\boldsymbol{I}_g = \boldsymbol{Z}_1^{-1}\Delta\boldsymbol{U}_1 \tag{28}$$

where $\Delta\mathbf{U}_1 = -\mathbf{B}_t\mathbf{Z}_{bt}\mathbf{T}_t^T\mathbf{I}_g$, and $\boldsymbol{Z}_1^{-1}$ is the inverse matrix of $\boldsymbol{Z}_1$.

Let the power source node voltage be $\mathbf{U}_0$, and the rest of each node voltage be $\mathbf{U}$ ($n\times1$-order matrix), then the voltage difference of either node and power source node equals to the sum of the branch voltages, which starts from this node, along the path to the power source node, that is

$$\Delta\mathbf{U}_{ti} = \mathbf{U}_0 - \mathbf{U}_i = \mathbf{T}_{ti}\mathbf{Z}_{\mathrm{bt}}\mathbf{I}_{\mathrm{bt}}, i = 1,2,...,n \tag{29}$$

where $\mathbf{T}_{ti}$, which is the row vector of corresponding path of node i in $\mathbf{T}_t$, is the path vector of node i.

6.2 Realization of power flow algorithm

Based on the above analysis, the specific steps of power flow algorithm for weakly meshed distribution network with different kinds of DGs are described below(k is the number of iterations).

Step 1: To calculate the path matrix $\boldsymbol{T}$ and loop-branch incident matrix $\boldsymbol{B}$ of weakly meshed distribution network. According to the power source node voltage, node voltage of each feeder line is then initialized.

Step 2: For different load models, to determine the relationship between load and voltage.

Step 3: PQ-type DG is treated as negative load, and reactive power of PI-type DG is determined by current. Reactive power of PQ(V)-type DG is determined by the functional relation of voltage and reactive power. For PV-type DG, the node reactance matrix of DG is built at first, then to determine the initial value of reactive power is based on the reactive power allocation principle, and to process PV node as PQ node.

Step 4: To calculate the injection current of each node. Let S_i be power injection of node i, and Y_i be sum of parallel admittance of node i, then we have

$$\bar{}_{\mathrm{g}i_k} = (\frac{i}{\bar{\mathrm{U}}_{\mathrm{i_{k-1}}}})^* - Y_i\overline{U}_{i_{k-1}} \quad i=1,2,\ldots,n. \tag{30}$$

Step 5: To calculate $\mathbf{f}_{1_k} = \mathbf{T}_t^T\mathbf{I}_{g_k}$ is based on Step 4.

Step 6: To calculate $\mathbf{I}_{\mathrm{bt}_k}$ is based on (26), then calculate $\mathbf{f}_{2_k} = \mathbf{B}_{t_k}^T\mathbf{I}_{1_k}$ based on (28).

Step 7: Calculating each node voltage $\mathbf{U}_{i_k} = \mathbf{U}_0 - \Delta\mathbf{U}_{ti_k}$, and $\Delta\mathbf{U}_{ti_k}$ is calculated by (29).

Step 8: To determine whether convergence. For non PV-type DG, the convergence condition is that the absolute value, which is the voltage amplitude difference between this and the last iteration, is not more than ε (ε is convergence precision), namely, $\max\left|U_i^{(k)} - U_i^{(k-1))}\right| \le \varepsilon$. For PV type node, if reactive power is beyond the limit, PV type node will be converted to PQ type node, on the contrary, judging by the voltage difference between this voltage value and the given one whether it is convergence, namely, $\max\left|U_i^{(k)} - U_s\right| \le \varepsilon$ (Us is the given voltage value of PV-type DG). If it is reached the scheduled accuracy, it will be convergence, then calculation ends, and outputs the results, otherwise, it is back to step 3.

The algorithm flow chart is shown in Fig. 5.

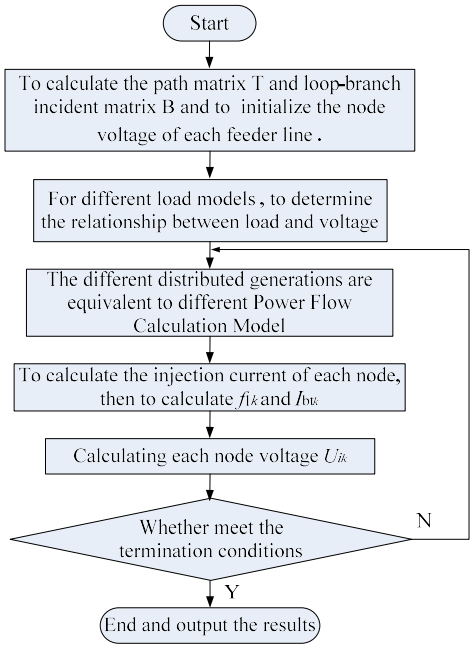

Fig. 5. Plow flow algorithm flow chart

7. Examples

In order to verify the effectiveness of the method proposed in this paper, the IEEE33 and PG&G69 nodes distribution systems are respectively used to perform the simulation test under the version of MATLAB2009a. In simulation, the two voltage levels are described by 12.66 kV, and the convergence accuracy is ε=10^{-4} [32].

7.1 Example 1

The IEEE33 node distribution system is shown in Fig. 6, which contains 33 nodes and 32 branches with the total active load being 3715kW and reactive power being 2300kvar, wherein 1 represents power source node as balance node, and DGs can installed in any nodes except the balance node.

1) Analysis of power flow calculation for weakly meshed distribution network without DG.

Without DG grid-connected, the results of power flow calculation of the three different algorithms are compared as shown in Table 1, which respectively is the algorithm proposed in this paper, and the one in [28], and the other

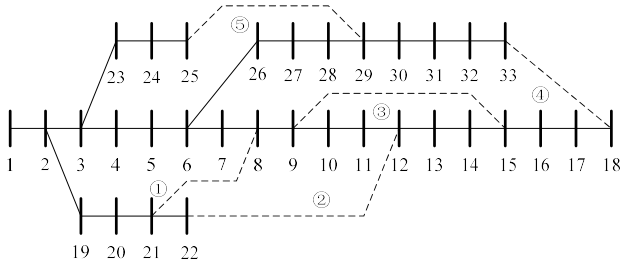

Fig. 6. IEEE33-node distribution system

Table 1. The results comparison between the proposed method and reference methods

Number of Ring Network	Closed Contact Line	Number of iteration		
		Proposed method in this paper	Proposed method in [28]	Proposed method in [33]
0		5	5	5
3	①②③	5	6	13
5	①②③④⑤	4	6	14

Table 2. Node voltage with weakly meshed system

node	voltage/pu	node	voltage/pu	node	voltage/pu
1	1.0000	12	0.9666	23	0.9957
2	0.9994	13	0.9597	24	0.9864
3	0.9986	14	0.9531	25	0.9770
4	0.9956	15	0.9508	26	0.9900
5	0.9941	16	0.9478	27	0.9889
6	0.9908	17	0.9417	28	0.9846
7	0.9856	18	0.9368	29	0.9769
8	0.9768	19	0.9983	30	0.9631
9	0.9727	20	0.9884	31	0.9515
10	0.9686	21	0.9854	32	0.9459
11	0.9680	22	0.9801	33	0.9436

in [33].

Table 1 shows the power flow calculation results of the three algorithms with different number of meshed networks. With the number of meshed network increasing from zero to five, the iteration times of the proposed algorithm reduces whereas the one of the other two increases. This is because of the shortened electrical distance from load to root node with closed loop, and the load voltage fluctuation diminished is caused by the change of load current such that the number of iterations are decreased. In [28] the adopted algorithm is the forward/backward sweep calculation, wherein the loops are firstly disconnected, and then calculate the breakpoint using compensation method, which will increase the complexity of program and iteration times, and lead to poor ability to deal with meshed network. In [33], the inner and outer loop calculation adopted will cause substantial increase of iteration times. In summary, the proposed method in this paper is more effective in solving the problem of the meshed network, and has better convergence performance and robustness.

Table 2 shows the node voltage magnitude as 5 loops are closed applying the method proposed in this paper. Comparing with the test results in [33], the voltage

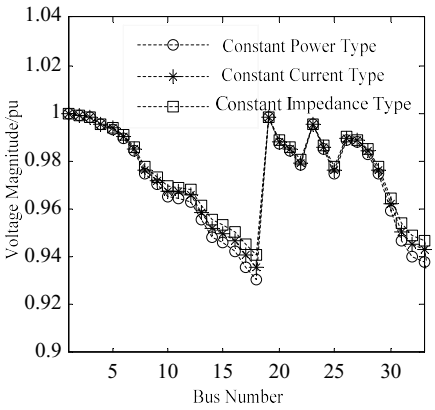

Fig. 7. Node voltage distribution with weakly meshed distribution network

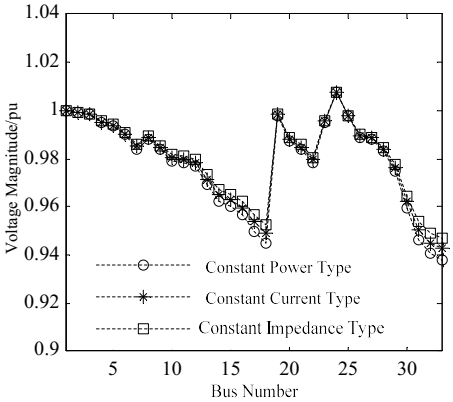

Fig. 8. Node voltage with PQ-type DG

magnitude elevates from 0.9165pu to 0.9368pu for node 18.

2) Influence analysis of static load characteristics

Fig. 7 shows the voltage distribution of weakly meshed distribution network under different load characteristics.

Seen from Fig. 7, without DG access, the each node voltage is slightly ascending with the load characteristic coefficients increasing, but this does not affect the iteration number of the algorithm, and the algorithm still possesses a good convergence. Under the influence of different load models, the node voltage at the end of the system changes more obviously. The reason lies in that when the voltage descends, the influence of static load characteristics on voltage stability increases, which results in the increased voltage variation of end node.

3) Simulation results of PQ type DG

Let 5 contact lines close, the PQ-type DG is respectively accessed in node 8 and 24. Active power output of each DG is 150kW, and reactive power is 150kvar. Each node voltage result is shown in Fig. 8.

Known from the simulation results, the system converges by four times iterations under the three models such as constant power, and constant current, and constant impedance load models, and their convergence time is

respectively 24.4ms, and 24.9ms, and 25.1ms. As shown in Fig. 8, the voltage decrease magnitude under constant impedance load model is the minimum, whereas that of constant power load is the maximum. In order to maintain constant power, the corresponding current has increased, which may lead to further decline in the voltage. Thus, for PQ-type DG, the different load models have an impact on voltage distribution.

4) Simulation results of PI-type DG

Let DG be accessed in the 8th and 30th nodes, with the active power of each DG being 150 kW, and the current 20A given. After the PI-type DG is accessed to system, the voltage distribution of each node is shown in Fig. 9.

Known from the simulations, for the constant power load model, the system converges after 5 iteration times with time cost 26.3 ms, whereas 6 times iterations for the constant current and constant impedance load model with the calculation time of 28.6 ms and 29.1 ms, respectively, which shows that the different static load characteristics have influence on convergence performance. The voltage amplitude of each node is generally above 0.96pu, the overall voltage level of system is improved. Thus, as PI-type DG is accessed to system, it provides reactive power to the system so as to improve the voltage level of the system.

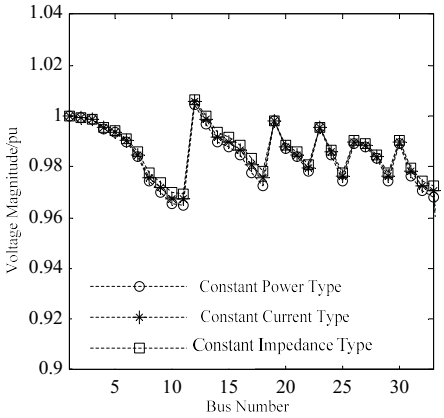

Fig. 9. Node voltage with PI-type DG

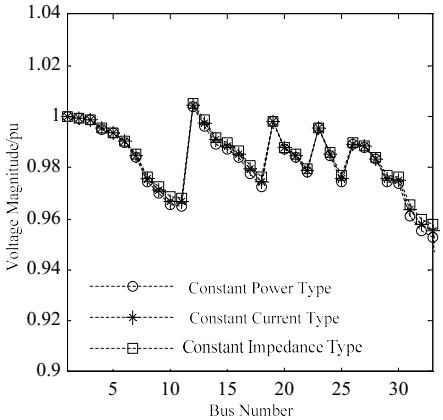

Fig. 10. Node voltage with PQ(V)-type DG

5) Simulation results of PQ (V)-type DG

Let PQ (V)-type DG be respectively connected to the nodes 12 and 26 with each active power output being 150kW, and x=0.5pu, and x_P=0.2pu. The node voltage distribution is shown in Fig.10.

The Fig. 10 shows that under the constant power and constant impedance load models, there are 5 times iterations required with calculation time respectively being 26.4 ms and 26.7 ms, whereas the iteration number under the constant current type is 6 times with calculation time is 27.2 ms. And due to accessing DGs in nodes 12 and 26, the voltages of the nearby nodes are also promoted.

6) Simulation results of PV-type DG

Let PV-type DGs be respectively connected in the nodes 8 and 30. The active power output of each DG is 150 kW with 12.66 kV given. The node voltage distribution is shown in Fig. 11.

Known from the simulation process, the iteration number of all the three kinds of load models under this condition is 6 times. And due to accessing DGs in nodes 8 and 30, the voltages of the nearby nodes are also improved.

Seen from the analysis, the algorithm adopted in this paper can effectively handle flow calculation for weakly meshed distribution network with PV type DG, and has good convergence. With the increasing coefficients of load characteristics, voltage level of the system is also improved.

7.2 Example 2

The PG&E69-node distribution system is shown in Fig. 12 [34], which contains 69 nodes and 73 branches with the total active load being 3802.2 kW and reactive power being 2694.6kvar, wherein contact switches are installed at lines between node 11 and node 66, 13 and 20, 15 and 69, 27 and 54, and as well as 39 and 48.

1) Analysis of power flow calculation for weakly meshed distribution network without DG.

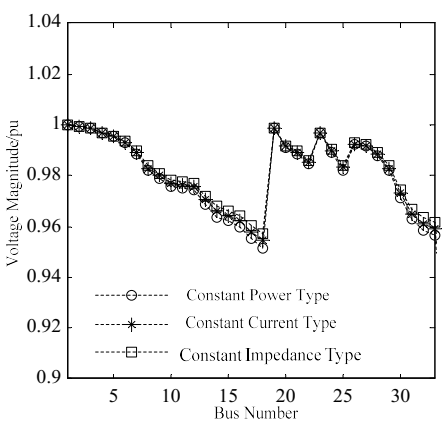

Fig. 11. Node voltage with PV-type DG

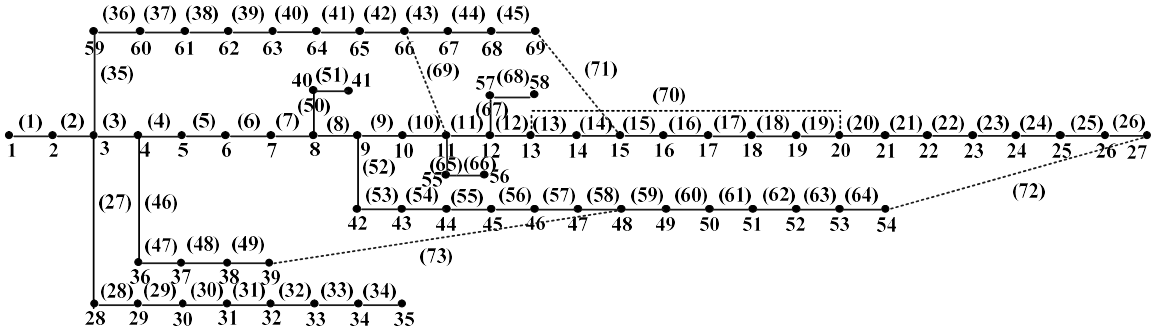

Fig. 12. PG&G69-node distribution system

Table 3. Node voltage with weakly meshed system

node	voltage/pu	node	voltage/pu	node	voltage/pu
1	1	24	0.9612	47	0.9615
2	0.9999	25	0.9575	48	0.9595
3	0.9999	26	0.9560	49	0.9534
4	0.9998	27	0.9552	50	0.9445
5	0.9993	28	0.9999	51	0.9445
6	0.9929	29	0.9998	52	0.9446
7	0.9863	30	0.9996	53	0.9451
8	0.9848	31	0.9995	54	0.9493
9	0.9840	32	0.9994	55	0.9771
10	0.9784	33	0.9990	56	0.9771
11	0.9772	34	0.9984	57	0.9722
12	0.9728	35	0.9983	58	0.9722
13	0.9690	36	0.9996	59	0.9998
14	0.9695	37	0.9949	60	0.9982
15	0.9702	38	0.9798	61	0.9967
16	0.9692	39	0.9764	62	0.9941
17	0.9677	40	0.9847	63	0.9840
18	0.9677	41	0.9847	64	0.9839
19	0.9668	42	0.9827	65	0.9796
20	0.9663	43	0.9812	66	0.9791
21	0.9640	44	0.9791	67	0.9790
22	0.9639	45	0.9772	68	0.9779
23	0.9631	46	0.9667	69	0.9779

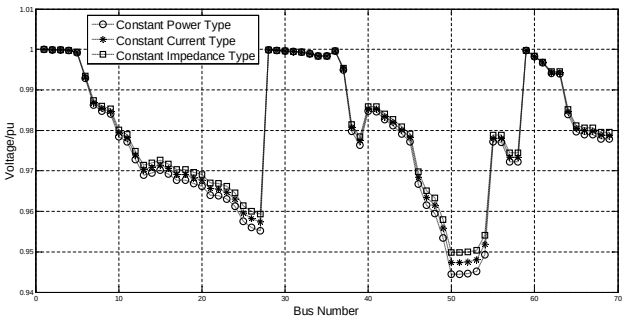

Fig. 13. Node voltage distribution with weakly meshed distribution network

Table 3 shows the node voltage magnitude when 5 loops are closed without DG access.

Considering static load characteristics, the voltage distribution of weakly meshed distribution network is shown in Fig. 13.

Known from the simulations, under the constant power, and constant current, and constant impedance load models, the system converges after 3 times iterations with calculation time respectively being 0.531664s, and 0.552896s, and 0.560586s. Fig. 13 shows that, without DGs, the voltage is slightly ascending with coefficient increasing of load characteristics, but this does not affect the number of iterations of the algorithm, such that the algorithm shows a good convergence. Under the influence of different load models, the node voltage at the end of the system changes obviously. The reason is that when the voltage is descended, the influence of static load characteristics on voltage stability increases, which results in the increased voltage variation of end node.

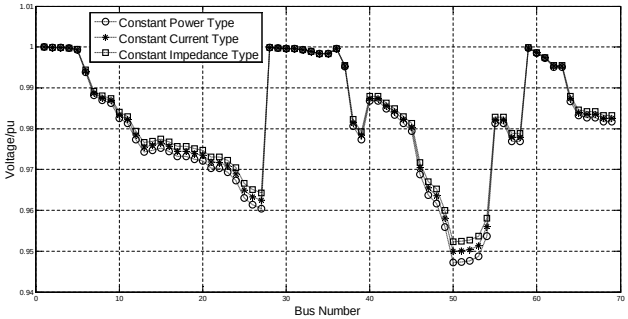

Fig. 14. Node voltage with PQ-type DG

2) Simulation results of PQ-type DG

Let five contact lines close, and PQ-type DG be respectively accessed in 10 and 22 nodes with active power output of each DG being 150kW and reactive power output be 150kvar. Each node voltage test result is shown in Fig.14.

From the simulation results, under the three load models such as constant power, and constant current, and constant impedance, the system converges via three times iteration with calculation time respectively being 0.629664s, and 0.647536s, and 0.651597s. In Fig. 14, the voltage decrease of constant impedance load model is the minimum, whereas that of constant power load is the maximum. This is since to maintain constant power, the corresponding current has increased, such that terminal voltage drops, which will lead to a further decline in the voltage. Thus, for

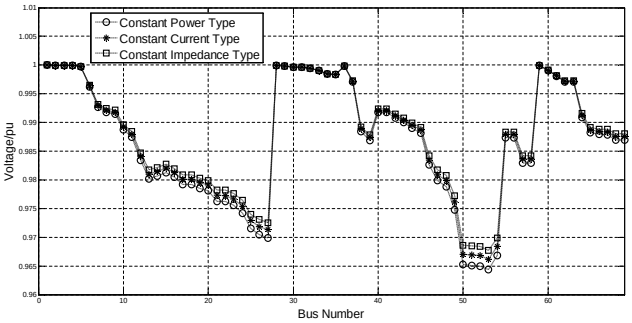

Fig. 15. Node voltage with PI-type DG

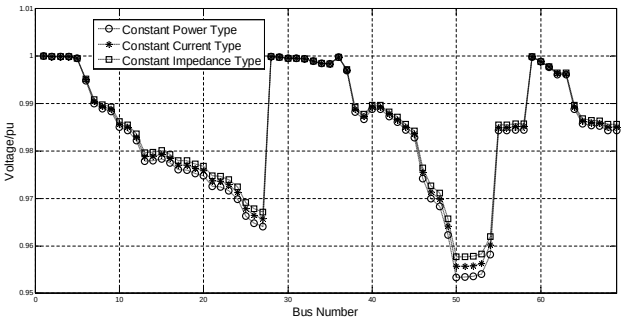

Fig. 16. Node voltage with PQ(V)-type DG

PQ-type DG, different load models have an impact on the level of voltage distribution.

3) Simulation results of PI-type DG

Let the DGs accessed in both 10 and 49 nodes, with the active power output of each DG being 150 kW and the current 20A given. After PI-type DG is accessed to system, the voltage distribution of each node is shown in Fig. 15.

According to simulations, the system converges after 3 times iteration for constant power load model, with the time being 0.568030s, whereas for the constant current and constant impedance load models there are 4 times iterations required, and the time cost being 0.574371s and 0.598730s, respectively. The voltage amplitude of each node is generally above 0.96pu, the overall voltage level of system is improved. Thus, when PI-type DG is accessed to system, it provides reactive power for the system to improve voltage level of the system.

4) Simulation results of PQ (V)-type DG

Let PQ (V)-type DG be respectively connected to the nodes 39 and 57 with each active power output being 150kW, and x=0.5pu, and x_p=0.2pu. The node voltage distribution is shown in Fig. 16.

Fig. 16 shows that for constant current and constant impedance load models, the system requires 4 times iterations with 0.742522s and 0.750226s, and the iteration number under constant power and constant current is 3 times with 0.674237s. Due to accessing DGs in nodes 39 and 57, the voltages of nearby nodes are promoted.

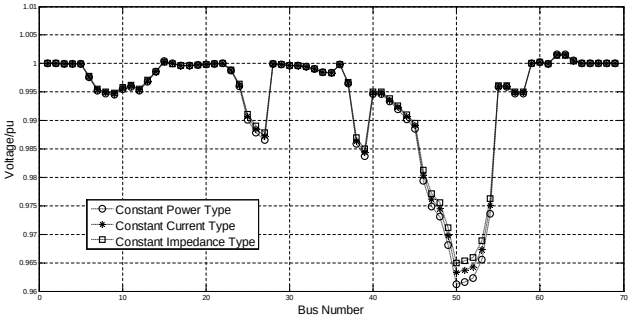

Fig. 17. Node voltage with PV-type DG

5) Simulation results of PV-type DG

Let PV-type DGs be respectively connected in the nodes 22 and 66. The active power output of each DG is 150 kW with 12.66 kV given. The node voltage distribution is shown in Fig. 17.

Known from the simulation process, the iteration number of all the three kinds of load models under this condition is 4 times. And due to accessing DGs in nodes 22 and 66, the voltages of the nearby nodes are also improved.

Clearly, we have similar results in the two examples, but the voltage level of the latter is better than the one of the former under same access DGs capacity, the reason lies in that the system scale of the latter is larger than the former, such that the disturbance aroused by DGs access is relatively small.

8. Conclusion

The algorithm proposed in this paper builds path-branch incident matrix and loop-branch incident matrix to process the power flow calculation containing the meshed network as DGs access based on loop-analysis method. The algorithm firstly establishes mathematical models of diverse types of DGs such as wind power, and photovoltaic cell, and fuel cell, and as well as gas turbine, which are respectively equivalent to diverse nodes such as PQ, and PI, and PQ (V), and as well as PV nodes. And then power flow calculations for distributed networks containing diverse types of DGs are restively implemented in IEEE33-node distributed system and PG&G69-node distributed system. The investigations show that with the load static characteristic value increasing, the voltage level of the system is improved after DG access, and this does not affect the times number of iterations of the algorithm, such that the algorithm possesses a good convergence. Under the influence of different load models, the node voltage at the end of the system changes, obviously. The test results can clearly reflects the influence of different load models on the system voltage level. The algorithm not only retains the advantage of high speed computing, but also possesses stronger dealing ability with meshed network. With the close loops number increasing, the

iteration times number of the algorithm will decreases. It is noted that the capacity of DGs access is far smaller than the one of the whole system loads but there one or several nodes where access DG capacity is greater than the load of the access node in this paper, according to analysis in section 2, under this situation the DGs access to distributed network will aim to improve the system voltage and reduce network loss. However, when the number of the DG access is more such tat its access capacity is far larger than the one of the system total load, according to description in section 2, the system voltage level may be degraded, this is our future research.

Acknowledgements

This research was financially supported by Science and Technology Program of Gansu Province (17JR5RA083) and Program for Excellent Team of Scientific Research in Lanzhou Jiaotong University（201701）

References

[1] S. Naka, T. Genji and Y. Fukuyama, "Practical Equipment Models for Fast Distribution Power Flow Considering Interconnection of Distributed Generators," *in Proceedings of IEEE/PES Summer Meeting*, Vancouver, Canada, July 2001.

[2] A P Agalgainkara, S V Kulkarni and S A Khaparde, "Evaluation of Configuration Plans for DGs in Developing Countries Using Advanced Planning Techniques," *IE*EE *Transactions on Power Systems*, vol. 21, no. 2, pp. 973-981, May 2006.

[3] Hossein Faraji, Farsam Farzadpour and Hamidreza Hajimirzaalian, "A New Hybrid Particle Swarm Optimization Approach for Sizing and Placement Enhancement of Distributed Generation," i*n Proceedings of the 4th International Conference on Power* Engineering, Energy and Electrical Drives, Istanbul, Turkey, May 2013.

[4] K. Moslehi and R. Kumar, "A Reliability Perspective of the Smart Grid," *IEEE Transactions on Smart Grid*, vol. 1, no. 1, pp. 57-64, June 2010.

[5] Yuan Zhaoxiang, Kong Xiangyu, Zhao Shuai, "Reliability Analysis Method for Distribution System with Distributed eneration," *Proceedings of the CSU-EPSA*, vol. 25, no. 4, pp. 112-116, Apr 2013.

[6] A. Keane, P Cuffe, E Diskine, and et al., "Evaluation of Advanced Operation and Control of Distributed Wind Farms to Support Efficiency and Reliability," *IEEE Transactions on Sustain Energy*, vol. 3, no. 4, pp. 735-742, Oct 2012.

[7] S. Gill, I. Kockar and G. W. Ault, "Dynamic Optimal Power Flow for Active Distribution Networks," *IEEE Transactions on Power Systems*, vol. 29, no. 1, pp. 121-131, Jan 2014.

[8] M. J. Dolan, E. M. Davidson and I. Kockar, "Distribution Power Flow Management Utilizing an Online Optimal Power Flow Technique," *IEEE Transactions on Power Systems*, vol. 27, no. 2, pp. 790-799, May 2012.

[9] M. M. A. Abdelaziz, H. E. Farag and E. F. E. Saadany, "A Novel and Generalized Three-phase Power Flow Algorithm for Island Micro-grids Using a Newton Trust Region Method," *IEEE Transactions on Power Systems*, vol. 28, no. 1, pp. 190-201, May 2013.

[10] Wang S and Wang C, Modern Distribution System Analysis. Beijing, Higher Education Press, 2007.

[11] Zhu X, Zhang J and Liu W, "Power Flow Calculation of Distributed System with Distributed Generation Considering Static Load Characteristics," *Power System Technolog*y, vol. 36, no. 2, pp. 217-223, Jan 2012.

[12] Ma Rui and He Renmu, "Research on Spot Pricing Approach Considering Load Static Voltage Characteristics," *Power System Technology*, vol. 30, no. 1, pp. 9-13, Jan 2006.

[13] S.Tong and K. Miu, "A Network-based Distributed Slack Bus Model for DGs in Unbalanced Power Flow Studies," *IEEE Transactions on Power Systems*, vol. 20, no. 2, pp. 835-842, May 2005.

[14] P. R. Bijwe and G. K. Viswanadha, "Fuzzy Distribution Power Flow for Weakly Meshed system," *IEEE Transactions on Power Systems*, vol. 21, no. 4, pp. 1645-1652, Nov. 2006.

[15] A. Losi and M. Russo, "Object-Oriented Load Flow for Radial and Weakly Meshed Distribution Networks," *IEEE Transactions on Power Systems*, vol. 18, no. 4, pp. 1265-1274, Nov. 2003.

[16] Zhang Qin, Zhou Buxiang and Lin Nan, "Improved Power Flow Algorithm for Distribution Networks Based on Zbus Algorithm and Forward/Backward Sweep Method," *Proceedings of the CSU-EPSA*, vol. 24, no. 6, pp. 73-77, Jun 2012.

[17] Yang Chao, Shen Cong and Li Rui, "Processing of PV Nodes in Forward/Backward Sweep Algorithm for Distribution Network Containing Distribution Generators," *Power System Technology*, vol. 36, no. 9, pp. 238-243, Apr 2012.

[18] S. X. Wang, X. Y. Jiang and C. S. Wang, "Power Flow Analysis of Distribution Network Containing Wind Power Generator," *Power System Technology*, vol. 30, no. 21, pp. 42-45, Nov 2006.

[19] H. Y. Chen, J. F. Chen and X. Z. Duan, "Study on Power Calculation of Distribution System with DGs," *Automation of Electric Power Systems*, vol. 30, no. 1, pp. 35-40, Jan 2006.

[20] Y. Zhu and K. Tomsovic, "Adaptive Power Flow Method for Distribution Systems with Dispersed Generation," *IEEE Trans. Power Del*., vol. 17, no. 3, pp. 822-827, Jul 2002.

[21] Chen Haiyan, Chen Jinfu and Duan Xianzhong, "Study on Power Flow Calculation of Distribution System with DGs," *Automation of Electric Power Systems*, vol. 30, no. 1, pp. 35-40, Jan 2016.
[22] Zhou J, Su H, "Back/Forward Sweep Power Flow Calculation with Distributed Generation Considering Static Load Characteristics," *Power System Protection and Control*, vol. 43, no. 24, pp. 26-31, Dec 2015.
[23] Ochoa L F, Padilla F A and Harrison G P, "Evaluating Distributed Generation Impacts with a Multi-objective Index," *IEEE Transactions on Power Delivery*, vol. 21, no. 3, pp. 1452-1458, Mar 2006.
[24] Li X, Peng Y and Zhao J, and et al., "Power Flow Calculation of Distribution Network with Distributed Generation," *Power System Protection and Control*, vol. 37, no. 17, pp. 78-81+87, Sep 2009.
[25] Jagaduri T and Radman G, "Modeling and Control of Distributed Generation Systems Including PEM Fuel Cell and Gas Turbine," *Electric Power Systems Research*, vol. 77, pp. 83-92, Feb. 2007.
[26] Cao Bin, "Parallel Computing of Three-phase Flow Calculation for Distribution System with Distributed Power," *Dissertation, North China Electric Power University*, 2014.
[27] Carson W. Taylor, Power System Voltage Stability, McGraw-Hill Companies, Inc, 1 994.
[28] Dai J, Wang S and Zhu J, "Power Flow Method for Weakly Meshed Distribution Network with Distributed Generation," *Power System Protection and Control*, vol. 39, no. 10, pp. 37-41, May 2011.
[29] Li T, Han Y and Hu X, "Characteristics of Static Voltage Stability for Distributed Generation Integrated into Power System and Its Impacts Analysis," *Power System Protection and Control*, vol. 42, no. 12, pp. 8-13, Jun 2014.
[30] Zhang L and Tang W, "Back/Forward Sweep Power Flow Calculation Method of Distribution Networks with DGs," *Transactions of China Electrotechnical Society*, vol. 25, no. 8, pp. 123-130, Aug 2010.
[31] Yan L, Xie Y and Xu J, "Improved Forward and Backward Substitution in Calculation of Power Distribution Network with Distributed Generation," *Journal of Xi'an University*, vol. 547, no. 6, pp. 117-123, Dec 2013.
[32] Xu Q, Liu Z and Yang Y, "Improved Method of Distribution Network Three-phase Power Flow Calculation," *Proceedings of the CSU-EPSA*, vol. 26, no. 9, pp. 23-29, Sep 2014.
[33] Li Z, "Power Flow Algorithm for Distribution Network with Distributed Generations," Dissertation, Zhenzhou University, 2012.
[34] Yang T, "Research of Distribution Network Reconfiguration Based on Tabu-Particle Swarm Optimization," *Dissertation, Lanzhou Jiaotong University*, 2014.

Hongsheng Su He received PhD degree in electrical engineering from Southwest Jiaotong University, Chengdu, China. His research interests are power system analysis, development and utilization of new energy, and etc.

Zezhong Zhang He received BS degree in electric engineering and automation from Hangzhou Dianzi University, Hangzhou, China. His research interests arepower system flow calculation, distributed network low-voltage gover-nance, and etc.